Food Hydrocolloids 35 (2014) 36–50

Contents lists available at ScienceDirect

Food Hydrocolloids

journal homepage: www.elsevier.com/locate/foodhyd

Electrospinning and heat treatment of whey protein nanofibers

Stephanie T. Sullivan [a], Christina Tang [a], Anthony Kennedy [b], Sachin Talwar [a], Saad A. Khan [a,*]

[a] Department of Chemical and Biomolecular Engineering, North Carolina State University, Raleigh, NC 27695-7905, USA
[b] Department of Chemistry, East Carolina University, Greenville, NC 27858, USA

ARTICLE INFO

Article history:
Received 29 March 2013
Accepted 22 July 2013

Keywords:
Whey protein
Nanofiber
Crosslinking
Electrospinning

ABSTRACT

The ability to develop nanofibers containing whey proteins presents a unique opportunity to exploit the inherent benefits of whey protein with that of the desirable attributes of nanofibers. In this study, aqueous whey protein solutions, both whey protein isolate (WPI) and one of its major components beta-lactoglobulin (BLG), are electrospun into nanofibers in conjunction with a spinnable polymer, poly(-ethylene oxide) (PEO). WP:PEO solution composition as high as 3:1 and with average fiber diameters ranging from 312 to 690 nm are produced depending on polymer composition and concentration. WP/PEO solutions are also successfully electrospun at acidic pH ($2 \leq pH \leq 3$), which could improve shelf life. FTIR analysis of WP/PEO fiber mat indicates some variation in WP secondary structure with varying WPI concentration (as WPI increases, % α-helix increases and β-turn decreases) and pH (as pH decreases from neutral (7.5) to acidic (2), % β-sheet decreases and α-helix increases). XPS also confirms the presence of WP on the surface of the blend fibers, augmenting the FTIR analysis. Interestingly, WP/PEO composite nanofibers maintain its fibrous morphology at temperatures as high as 100 °C, above the 60 °C PEO melting point. In addition, the mats swell in water and retain a fibrous quality which makes them desirable for application in regenerative medicine. Finally, we incorporate a small hydrophobic molecule Rhodamine B (RhB) as a model flavonoid into WP/PEO nanofiber mats. The BLG:PEO nanofibers qualitatively exhibit improved fiber quality and RhB distribution compared to PEO nanofibers; however, no effect on the release profile is observed.

© 2013 Elsevier Ltd. All rights reserved.

1. Introduction

Whey proteins, one of two milk protein groups along with the caseins, have been found to be a valuable dietary supplement and a functional food enhancer. Whey proteins are used in food design due to the variety of functionalities including: binding of water and flavor, gelation, emulsification and foaming (Chandan, 2006; Chandan & Shah, 2006). Furthermore, whey proteins are being evaluated and recognized for their antimicrobial, antiviral, and anticarcinogenic effects (Chatterton, Smithers, Roupas, & Brodkorb, 2006; Ha & Zemel, 2003; Madureira, Pereira, Gomes, Pintado, & Malcata, 2007). The predominant whey proteins, β-lactoglobulin (BLG) and α-lactalbumin (ALA), are globular proteins with an isoelectric point of approximately 5.2 and 4.3, respectively (Eissa & Khan, 2005). The most abundant bovine milk protein, native BLG has 162 amino acid residues, eight anti-parallel β-sheets, one α-helix chain and a molecular weight of 18 kDa (Jung, Savin, Pouzot, Schmitt, & Mezzenga, 2008); while ALA has 123 amino acid residues, a secondary structure consisting of α-helix (~31%), 3_{10}-helix (~21%) and a small contribution of β-strands (~6%) (Alting et al., 2004), and a molecular weight of 14 kDa (Eissa & Khan, 2005).

A significant fraction of whey protein research has focused on gelation and gel characteristics (Bertrand & Turgeon, 2007; Daubert, Hudson, Foegeding, & Prabhasankar, 2006; Eissa, Bisram, & Khan, 2004; Eissa & Khan, 2006; Errington & Foegeding, 1998) because these gels can provide food products with unique functional performance and favorable textural properties. Recently, structures made from milk proteins such as whey have been recognized as an important tool in vehicles for the delivery of bioactives and pharmaceuticals (Livney, 2010; MaHam, Tang, Wu, Wang, & Lin, 2009; Satpathy & Rosenberg, 2003). Nanofibers, in particular, are considered promising for drug delivery due to their high specific surface area leading to efficient drug release (Cui, Zhou, & Chang, 2010; Ignatious & Sun, 2006; Ignatious, Sun, Lee, & Baldoni, 2010; Srikar, Yarin, Megarides, Bazilevsky, & Kelley, 2008). Nanofiber structures of whey protein may be especially well suited for such applications.

* Corresponding author. Tel.: +1 919 515 4519.
E-mail address: khan@eos.ncsu.edu (S.A. Khan).

0268-005X/$ – see front matter © 2013 Elsevier Ltd. All rights reserved.
http://dx.doi.org/10.1016/j.foodhyd.2013.07.023

Electrospinning is a simple process used to produce nanofibers, in some cases smaller than 100 nm in diameter (Frenot & Chronakis, 2003). Equipment for two electrospinning methods, melt and solution electrospinning, have been thoroughly discussed in the literature (Frenot & Chronakis, 2003). Solution electrospinning utilizes polymer dissolved in solvent that is pumped at a controlled flow rate from a syringe to which a high voltage is applied. Electrostatic forces between the positively charged syringe needle and a grounded collector plate pull solution away from the syringe tip into a Taylor cone formation and to the collector. As the solution is pulled away from the syringe, the solvent evaporates, leaving the polymer drawn into fibers and collected as a fiber mat (Andrady, 2008; Huang, Zhang, Kotaki, & Ramakrishna, 2003; Li & Xia, 2004; Saquing, Manasco, & Khan, 2009). Solution electrospinning allows for encapsulation of insoluble particles within a nanofiber mat and the incorporation of soluble drugs in a uniform fashion (Frenot & Chronakis, 2003). Nanofiber systems also can serve as wound healing dressings (Katti, Robinson, Ko, & Laurencin, 2004) or as a scaffold for tissue engineering (Boudriot, Dersch, Greiner, & Wendorff, 2006; Li, Laurencin, Caterson, Tuan, & Ko, 2002). Other nanofiber designs include modifying the nanofiber surface with nanoparticles (Saquing et al., 2009) bioactive peptides and proteins (Choi & Yoo, 2007; Sun, Shankar, Börner, Ghosh, & Spontak, 2007) and immobilizing enzymes (Jia et al., 2002). Electrospun biopolymer nanofibers have also been highlighted as a novel tool for food industry applications such as nutraceutical and flavor release (Kriegel, Arrechi, Kit, McClements, & Weiss, 2008).

Some milk proteins have been utilized in solution electrospinning. Bovine serum albumin, for example, has been successfully electrospun both with (Jiang et al., 2005; Kowalczyk, Nowicka, Elbaum, & Kowalewski, 2008; Zeng et al., 2005) and without (Dror et al., 2008) the use of a carrier polymer; while caseins yielded successful nanofibers only when blended with spinnable polymer (Xie & Hsieh, 2003). Nanofibers have also been obtained from other proteins including silk fibroin (Jin, Fridrikh, Rutledge, & Kaplan, 2002; Kim, Nam, Lee, & Park, 2003; Min et al., 2004), zein (Miyoshi, Toyohara, & Minematsu, 2005), keratin (Zoccola et al., 2007), collagen (Li et al., 2005; Yang, Ichii, Murase, & Sugimura, 2012), fibrinogens (Wnek, Carr, Simpson, & Bowlin, 2003), egg protein (Wongsasulak, Kit, McClements, Yoovidhya, & Weiss, 2007; Yi, Guo, Fang, Yu, & Li, 2004), and wheat protein (Woerdeman, Shenoy, & Breger, 2007; Woerdeman et al., 2005). However, neither of the two primary whey proteins BLG and ALA nor a commonly utilized combination of the two – whey protein isolate (WPI) have been electrospun into nanofibers. This is important because the ability to electrospin nanofibers that contain whey proteins could combine the unique attributes of whey proteins with those that nanofibers offer. For instance, whey protein nanofibers can be envisaged for texture modifier in chocolate while providing nutritional value. Nanofibers are also being considered for drug delivery and tissue scaffolds, and the biocompatibility and biodegradable aspects of whey proteins make it a viable candidate in these applications. Further, we may be able to exploit the ability of BLG to form covalent crosslinks with heat to achieve water-insoluble mat. This eliminates the need to electrospin from harmful solvents or chemical crosslinkers. Heat-induced crosslinking of electrospun WP fibers by this method makes our system unique, producing nutrient-loaded water-insoluble, biocompatible nanofibers.

In this study, we examine strategies to make nanofibers with whey proteins and enhance these whey protein-based fibers with changes in concentration, pH, addition of a hydrophobe and heat-induced crosslinking. We address critical issues such as whether whey proteins can be electrospun into nanofibers in their native, chemically or heat denatured forms; or must they, similar to the caseins, be solution electrospun with a carrier polymer (Xie & Hsieh, 2003). The globular nature of whey proteins such as BLG and ALA, the low viscosity of their aqueous solutions, and potential lack of molecular entanglement makes producing nanofibers challenging (Nie et al., 2008; Woerdeman et al., 2007). The addition of spinnable polymer may be required, as was executed with other proteins such as egg proteins (Wongsasulak et al., 2007; Yi et al., 2004). We also explore the effect of solution pH on electrospinning, as it influences whey protein solution behavior (Eissa & Khan, 2005). Further, changing the pH of the solution expands the ability to incorporate drugs or flavonoids. Electrospinning aqueous whey protein solutions at acidic pH would facilitate formulation flexibility and improved shelf life (International Commission for the Microbiological Specifications for Foods, 1998). In order to improve the stability of the fibers, we examine covalent crosslinking by heat treatment as whey protein can be heat denatured (Anema, 2008) at approximately 70 °C when it forms disulfide bonds between neighboring chains. Finally, we incorporate and monitor the release of a fluorescent dye as a model hydrophobic molecule.

2. Materials & methods

2.1. Solution preparation

BiPRO Whey Protein Isolate (WPI) and BIOPURE β-lactoglobulin (BLG) were both obtained from Davisco Foods Inc. (Eden Prairie, MN) and uses as received (98% protein). Some BIOPURE BLG was purified (Mailliart & Ribadeau-Dumas, 1988) and verified with NuPAGE. Poly(ethylene oxide) (PEO) Polyox WSR205 (MW 600 kDa, Polydispersity Index 12 (Little & Ting, 1976)) was obtained from The Dow Chemical Company (Midland, MI) and used as received. Hydrochloric acid, ethanol, urea and Rhodamine B were used as received from Sigma. WPI, BLG, and PEO were dissolved in deionized water (DW) and stirred for a minimum of 3 h to ensure complete dissolution. Solution pH and conductivity were measured with a Fisher Scientific Accumet AB15 pH meter and Accumet AB30 conductivity meter, respectively. The viscosities of pertinent samples were measured at 25 °C in a TA Instruments AR-2000 stress controlled rheometer using a cone and plate geometry.

2.2. Solution electrospinning

The electrospinning apparatus, described previously (Saquing et al., 2009) included a precision syringe pump (Harvard Apparatus, Holliston, MA) operated at flow rate of 0.1–2.0 ml/h, and a high-voltage power supply (Gamma High Voltage Research, model D-ES30 PN/M692 with a positive polarity between 0 and 30 kV) Electrospinning solutions were loaded in a 10 ml syringe to which a stainless steel capillary metal-hub needle (22 gauge) was attached. The positive electrode of the high voltage was connected to the needle tip. The grounded electrode was connected to an aluminum foil-covered metallic collector (Talwar, Hinestroza, Pourdeyhimi, & Khan, 2008). The tip-to-collector distance varied from 12 to 17 cm.

2.3. Morphology & surface analysis

Specimens from solution electrospinning experiments were mounted on stubs; sputter coated with ~15–40 nm layer of gold and examined using scanning electron microscopy (SEM, FEI Quanta 200 Environmental Scanning Electron Microscope). Fiber size distributions were obtained by measuring a minimum of 100 fibers using Image J software (NIH). A Riber X-ray Photoelectron Spectrometer (XPS) operated at 12 kV with a 1 mm spot size was used for nanofiber mat surface analysis. Differential scanning calorimetry (DSC) was utilized (TA Instruments, DSCQ200, New

Castle, DE) to analyze fiber mat thermal properties at a heating rate of 10 °C/min under inert Argon gas.

The infrared spectra of nanofiber mats were recorded at room temperature using a Nicolet Magna-IR 750 spectrometer (Madison, WI). Dry air was continuously run through the spectrometer. The infrared spectra were recorded at 2 cm^{-1} resolution. A total of 128 transmission scans were recorded, averaged, and apodized with the Happ-Genzel function. Additional Infrared spectra were obtained on a Nicolet 6700 FTIR (Thermo Scientific, Madison WI) equipped with a DTGS detector and continually purged with dry air. Samples were analyzed directly on a single bounce diamond ATR (45°) by acquiring 128 scans at 4 cm^{-1} resolution at ambient temperature. Spectra were corrected for water vapor and then ATR corrected using the advanced ATR correction routine (Omnic 8.0) prior to secondary structure analysis. Secondary structure analysis was performed by using a curve resolution technique and determining the areas of the individual components. Band positions were confirmed with Fourier self deconvolution and also by obtaining second derivative spectra.

Confocal laser scanning microscopy (CLSM) fluorescent images were taken with a FV 300 scanner of the Olympus BX-61 system, equipped with high-resolution DP70 digital charge coupled device (CCD) camera (Olympus America Inc.) with objective magnifications ranging from 4× to 50×. Two and three dimensional LSM nanofiber images were taken with the Olympus LEXT OLS4000 confocal laser scanning microscope metrology system. Reflected light microscope images were taken with an Olympus BX-51 microscope system with objective magnifications ranging from 10× to 100×. Release studies were conducted directly in deionized water-filled cuvets. Readings were taken every two minutes using a Perkin Elmer Lambda 45 Spectrometer at 543 nm (Waltham, MA).

3. Results and discussion

3.1. Electrospinning WP/PEO blends

We hypothesize that whey proteins in their native or denatured state do not have sufficient entanglement or interactions (such as cyclodextrins (Manasco, Saquing, Tang, & Khan, 2012)) to electrospin. This is based on the premise that our initial attempts to electrospin WPI or BLG at various concentrations, either in native or denatured state, yielded micro and nanoparticles but no nanofibers (Supplementary Fig. 1). Details of these experiments and corresponding microstructures are presented in Supplementary data. So in the next set of experiments we blended WPI with a water soluble, electrospinnable polymer, polyethylene oxide (PEO), to attempt to facilitate fiber formation (Kowalczyk et al., 2008; Xie & Hsieh, 2003). As shown in Fig. 1, these WPI/PEO blends successfully yielded nanofiber mats, and a maximum of 75 w/w% whey protein was achieved. Interestingly, at 4 w/w% PEO produces beaded fibers (Fig. 1(a)), but the addition of the WPI (maintaining 4 w/w% PEO) leads to uniform bead-free fibers. As expected, the fiber diameter increases as the total polymer (protein and PEO) concentration increases, but the process parameters also play a role in uniformity. For example, WPI:PEO 50:50 and 60:40 mats are very close in mean diameter. Both were electrospun with a 15 cm tip-to-collector distance, 1 ml/h flow rate and 22 gauge 2 inch needle, but the 60:40 utilized a higher voltage (10 kV vs. 9 kV). The stronger electrostatic force of the higher 10 kV could explain the slightly smaller fibers achieved at a higher concentration. However, the 50:50 WPI/PEO fiber mats had a mean fiber diameter of 321 ± 56 nm with the lowest standard deviation, thus the most uniform fibers produced. This result agrees with qualitative assessment that the fibers were less uniform both above and below the 8 total w/w%. Fibers with the highest WPI concentration are somewhat less uniform in diameter and even "wavy" in appearance, with a higher mean diameter and standard deviation (668 ± 135 nm) with some minor fiber breakage present (Fig. 1(e)).

We also electrospun blends of BLG and PEO at different ratios holding the total weight of polymer in solution constant (10 w/w%) to determine the impact of changing the relative amount of the two constituents (Fig. 2). We used BLG instead of WPI to examine if we could achieve consistent results between the two in terms of electrospinnability. At various blend ratios, the nanofibers appeared to be commensurate with respect to total polymer weight, with mean diameters ranging from 381 to 466 nm. Comparing the 75:25 BLG/PEO blend with the WPI/PEO blend, total polymer concentration of 10 and 16 w/w%, respectively, the BLG/PEO blend fibers did not appear to have issues of "waviness" or breakage. This could be due to the decreased total polymer concentration or solution homogeneity with BLG in lieu of the mixture of proteins in the WPI formulation. In addition, the fiber diameters are smaller because of the lower polymer concentration.

3.2. Effect of pH on whey protein/PEO electrospinning

The use of whey proteins at acidic pH is often desirable for reduced bacterial growth and increased product shelf life (Woerdeman et al., 2007). For example, for food applications which would benefit from control release or texture functionality of fibrous mats, minimizing bacterial growth by its acidic or alkaline composition would improve shelf life. Alternatively, tissue scaffolds comprised of nanofiber mats that could be prepared and packaged/stored for use as needed on battlefields or in hospitals would benefit from improved shelf life that has potential to be controlled by pH. Acidic whey protein gels have been well studied for food applications (Eissa & Khan, 2006). Therefore, we electrospun acidic whey protein/PEO solutions. However, previous results indicate that pH of the solution affects the electrospinning process due to changes in solution conductivity (Son, Youk, Lee, & Park, 2005; Song, Kim, & Kim, 2008). For example, Son et al. (2005) investigated the effect of pH variation (from 2 to 12) on poly(vinyl) alcohol electrospinning. Beaded nanofibers were obtained under acidic conditions whereas finer, defect-free fibers resulted from basic solutions. Further, pH also affects the structure and net charge of proteins. For example, whey proteins are known to extensively aggregate at pH near their isoelectric points. Changes in pH of the electrospinning solution are expected to affect fiber morphology as previously reported with zein, and the effect of pH on protein electrospinning is likely protein dependent (Torres-Giner, Gimenez, & Lagaron, 2008; Zhu, Shao, & Hu, 2007). In our case, we examine electrospinning whey protein and PEO at acidic pH no lower than 2.0 to avoid polymer degradation (Song et al., 2008).

To examine the effect of blend composition on nanofiber characteristics at low pHs using WPI, we used a total polymer concentration of 5.5 w/w%. Fig. 3 shows SEMs of each electrospun fiber mat (Fig. 3(a)–(d)) and provides information on the precursor solution concentrations, pH, zero shear viscosity and mean nanofiber diameter (Fig. 3(e)). Several features are apparent from the data. First, we find all four solutions of PEO:WPI ratios ranging between 50:50 and 80:20 produced bead-free nanofibers. Secondly, these nanofibers exhibit similar diameters between 262 and 312 nm even though the viscosity changes greatly (by a factor of seven). In the case of the low pH studies shown in Fig. 3, substitution of WPI for PEO in the total 5.5 w/w% solutions increased conductivity of the samples from ~0.1 mS/cm for a 100% PEO solution to 1.5 mS/cm for the 80:20 PEO:WPI sample, and again to 3.4 mS/cm for the 50:50 PEO:WPI sample. These results suggest that fiber diameter is not being solely dictated by polymer concentration or viscosity. A

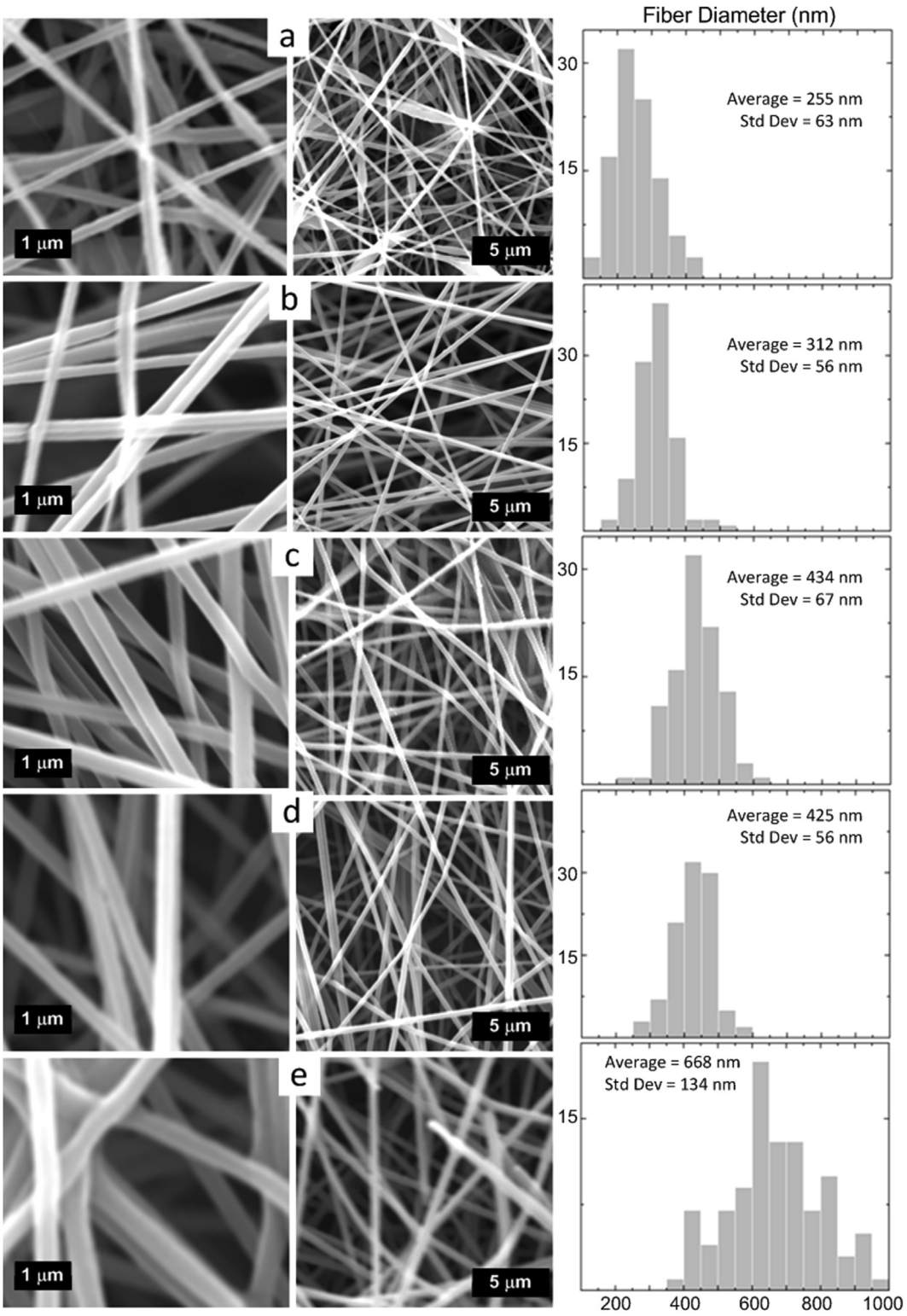

Fig. 1. Scanning electron micrographs and fiber diameter analysis of whey protein isolate (WPI) and poly(ethylene oxide) (PEO) blend solution electrospun nanofibers. PEO 4 w/w% with increasing WPI (and thus total weight) concentration, with WPI:PEO ratio (a) 0:100; (b) 40:60; (c) 50:50; (d) 60:40; (e) 75:25.

statistical difference between the mean nanofiber diameter is not apparent, but may be due to the variation in electrospinning applied voltage (the applied voltage for the 66:34 solution was 9.5 kV whereas that for the 80:20 solution was 11.0 kV) or due to the globular nature of the protein in that inter-chain entanglements did not increase at this acidic pH where the whey protein exists in a monomer state. Other work by Son, Youk, Lee, and Park (2004) revealed that addition of a polyelectrolyte to PEO decreased fiber diameter to a constant value, with a concomitant increase in conductivity. However, further addition of polyelectrolyte did not change the fiber diameter but increased conductivity monotonically. We believe our results are consistent with this scenario.

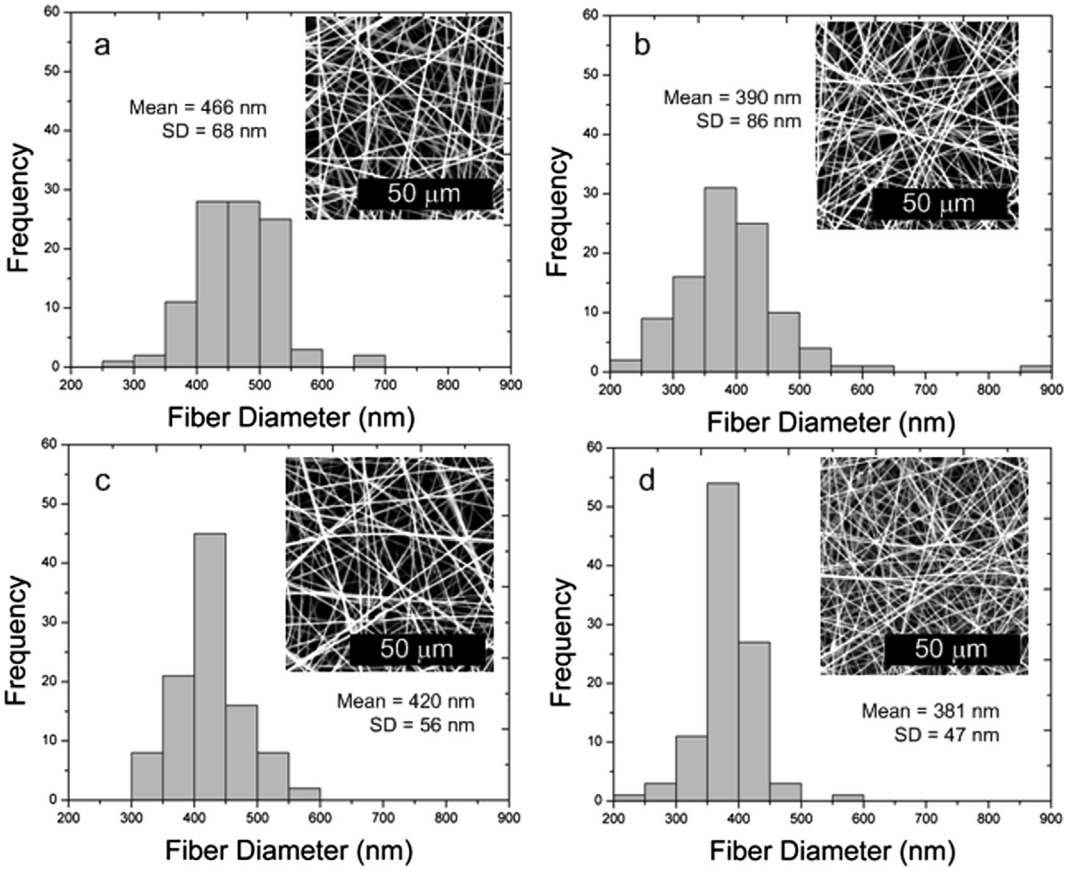

Fig. 2. Scanning electron micrographs and fiber diameter analysis of β-lactoglobulin (BLG) and poly(ethylene oxide) (PEO) blend solution electrospun nanofibers. Fibers spun at 15 cm tip-to-collector distance and 22 gauge needle. Total 10 w/w% with BLG:PEO ratio (solution viscosity Pa s; flow rate ml/h; voltage) (a) 75:25 (0.5; 1.0; 9.5 kV); (b) 60:40 (3.2; 0.5 ml/h; 10.5 kV); (c) 50:50 (10; 0.2 ml/h; 10 kV); (d) 40:60 (23; 0.1 ml/h; 15 kV).

We also studied the effect of pH on BLG/PEO blends (Fig. 4). We used BLG instead of WPI to be able to better analyze the results in terms of the isoelectric point of a single protein. Solutions of 50:50 BLG and PEO were prepared at total 7 w/w% for pH of 7.5 (native solution pH), 5.2 (isoelectric point of BLG), 4.0 (near isoelectric point of ALA and other whey proteins in WPI), and acidic 2.0. Solutions at pH 7.5 and 2.0 were transparent and yellow in color; whereas solutions at pH 5.2 and 4.0 were milky white, indicating protein aggregation as expected. Conductivity of the solutions increased with decreasing pH (Fig. 4(g)), as expected, since BLG becomes more positively charged as the solution pH changes from 7.5 to 2.0. Solution viscosity was also affected by pH (Fig. 4(e)); it was lowest for pH 2.0 solution, likely due to the BLG being in a monomer state compared to the other three solutions. Also, pH 5.2 solution viscosities are slightly higher than other solutions, likely due to the impact of the BLG aggregation at its isoelectric point. Interestingly, work by Vega-Lugo et al. with a WPI–PEO system show higher viscosities at low and high pH which they attribute to the unfolded protein entangling more with PEO at these non-neutral environments (Vega-Lugo & Lim, 2012). They also observed no change in conductivity. The differences in our results could be due to the use of different materials and measurement conditions in the two studies.

At pH 7.5 and 2.0, uniform fibers are produced (Fig. 4(a) and (d), respectively). When the average fiber diameter at pH 7.5 and 2.0 are compared (453 nm–391 nm, respectively), the trend of decreasing fiber diameter with increasing solution conductivity agrees with that found in the literature (Bertrand & Turgeon, 2007). However, the pH 5.2 (Fig. 4(b)) and 4.0 (Fig. 4(c)) fibers both contain bead defects (~1 μm in diameter), possibly due to whey protein agglomeration in the solution. Viscosity does not appear to play a strong role in fiber quality in this case compared to the influence of protein aggregation and/or structural state.

3.3. WPI/PEO blend fiber analysis

FTIR analysis of the PEO and WPI/PEO blend fiber mats were conducted to confirm that both the PEO and WPI are present in the blend fiber mats as well as obtain information regarding the structure of the protein in the fiber. Spectra for all of the sample compositions shown in Fig. 1(a)–(e) were collected and were similar. A representative blend fiber mat spectra is shown in Fig. 5(a) for comparison to raw materials. Spectra for the WPI/PEO blend fiber mats show broad new bands at approximately 3280 cm^{-1}, 1650 cm^{-1}, and 1530 cm^{-1} compared to the PEO fiber and PEO powder spectrum. The 3280 cm^{-1} peak may represent NH stretching intensity that increases with molecular weight, while the 1650 cm^{-1} band, which is found in proteins, is assigned to the Amide I band. This combination band arises due to C=O stretching vibrations coupled to N–H and C–N vibrations. The band that appears at approximately 1530 cm^{-1} is assigned as the Amide II band which arises primarily due to N–H in-plane bending vibrations (Socrates, 1994). All of these are indicative of the presence of protein or more specifically in this case the whey protein isolate, which as noted before is primarily BLG and ALA. Previous FTIR analyses of BLG (Eissa, Puhl, Kadla, & Khan, 2006) reveal different structural characteristics (e.g., β sheets, α helices) of BLG in the 1600–1700 cm^{-1} range. The WPI/PEO fiber peak at 1650 cm^{-1} obtained

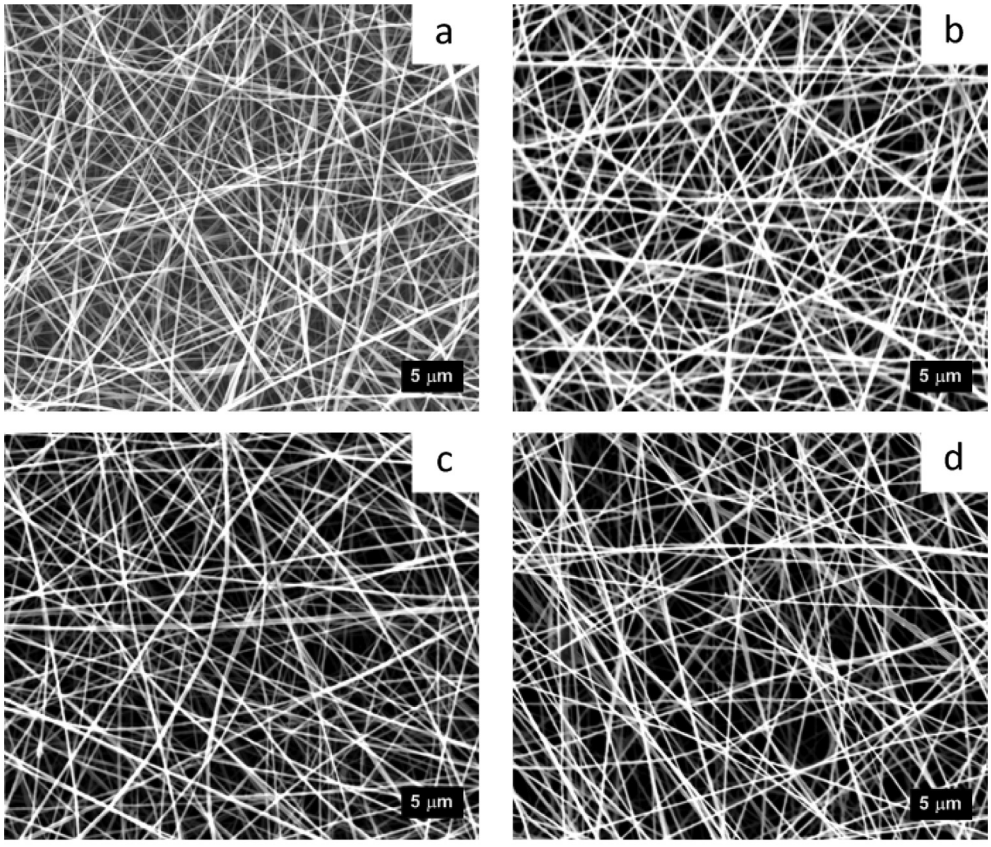

e

PEO:WPI ratio	PEO concentration (w/w%)	Solution pH	Solution viscosity (Pa s)	Nanofiber mean diameter* (nm)	standard deviation* (nm)
50:50	2.7%	2.36	0.34	312	69
57:43	3.2%	2.43	0.65	301	52
66:34	3.6%	2.55	1.04	304	51
80:20	4.4%	2.92	2.33	262	44

Fig. 3. Scanning electron micrographs of total weight 5.5 w/w% PEO:WPI acidic blend mats (a) 50:50, (b) 57:43, (c) 66:34 and (d) 80:20 by weight blend solution electrospun nanofiber mats produced. (e) provides solution and nanofiber data, with *nanofiber data determined from NIH Image J analysis with minimum 100 measurements.

from our samples is broad across this range, indicating that BLG may be present in some or all of these conformations. Eissa et al. also discussed that a change occurred in the magnitude of the spectra with increasing BLG concentration, although the shape of the spectra were similar (Eissa et al., 2006). Slight shifts in band position between very low (i.e., 0.25%) and the higher concentrations (3–7%) indicated that some molecular interaction may be influencing results with increasing concentration (Eissa et al., 2006). Our data also indicates a slight shift with overall whey protein concentration.

ALA, another protein in WPI, also absorbs in the 1610–1700 cm^{-1} region, as would be expected (Zhong, Gilmanshin, & Callender, 1999). Wongsasulak et al. (2007) found pure PEO electrospun nanofiber characteristic peaks at ~2900 (methylene group CH_2 molecular stretching), and at 1100 cm^{-1} and 958 cm^{-1} (C–O–C group stretching), which agrees with the PEO fiber peaks seen in our data (Fig. 5). A change in bandwidth for the absorption centered around 2880 cm^{-1} also occurs and increases with WPI concentration, thus decreasing with relative PEO concentration, which agrees with Eissa's observation of peak shifts with whey protein concentration (Eissa et al., 2006). We would expect this also due to more contributions and resultant heterogeneity of the WPI in the solution and resultant mat. Zeng et al. (2005) used FTIR to evaluate PVA/BSA fibers, concluding that BSA, which is classified as a whey protein, generated FTIR peaks at 1710 cm^{-1} and 1665 cm^{-1} representing amide bonds from BSA. The WPI/PEO fibers are not

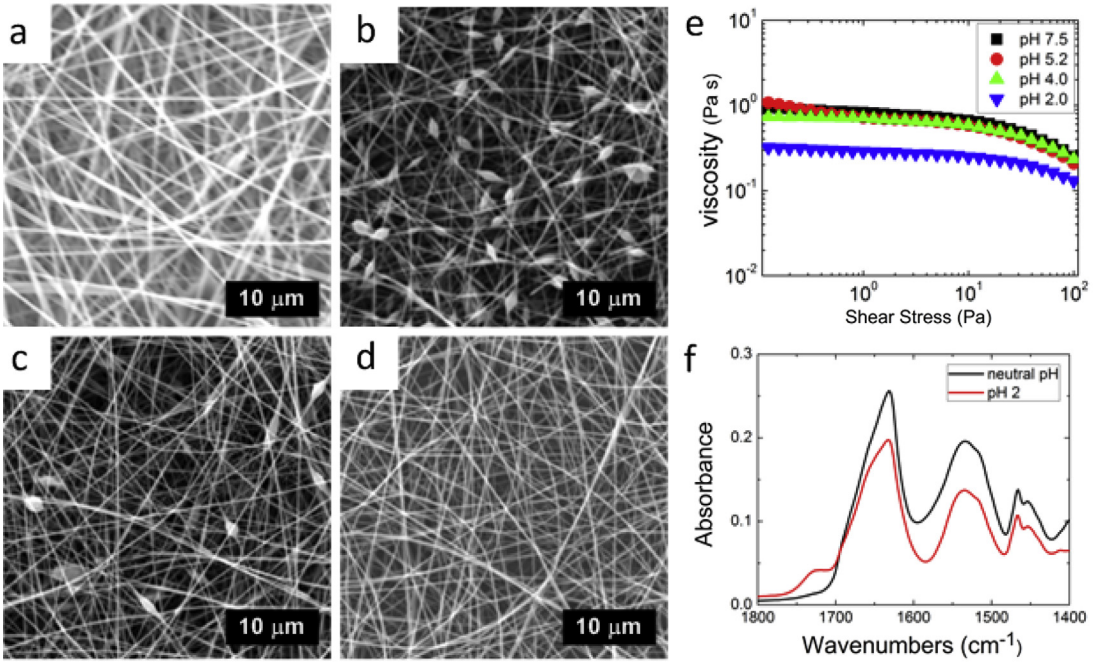

g

Solution pH	Solution Conductivity (mS/cm)	Nanofiber mean diameter (nm)	standard deviation (nm)	XPS Elemental Fiber Mat Content (%)				
				O	C	N	Cl	Na
7.5	2.5	453	82	24.62	63.84	11.27	0	0.28
5.2	3.8	Bead defects		28.42	62.01	9.35	0	0.23
4	5.6	Bead defects		*				
2	12.6	391	94	26.69	62.07	9.65	1.32	0.27

Fig. 4. Scanning electron micrographs of solution electrospun nanofibers from total 7 w/w% solution of 50:50 purified BLG:PEO at pH (a) 7.5; (b) 5.2; (c) 4.0, (d) 2.0. (e) shows solution steady shear viscosity vs. shear stress; (f) provides FTIR comparison of 50:50 WP:PEO fiber mat prepared from neutral pH and acidic pH 2; and (g) provides mean nanofiber diameter, X-ray photoelectron spectroscopy (XPS) and solution data for these mats of varying pH. Fiber mats at pH 5.2 and 4.0 each contained bead defects. For example, fibers formed with pH 5.2 solution had bead defects with measured average diameter of 1 μm. *Note that XPS was only completed on fiber mats of pH 2, 5.2 and 7.5.

expected to show a dominant BSA representation, as WPI was processed to approximately a 98% protein concentration using ionic exchange chromatography which retained the BLG and ALA; thus, BSA should not be present in significant quantities in the WPI/PEO fiber mats. Rather, our WPI/PEO fiber mat FTIR data is dominated in this range by the ALA.

Where possible, secondary structural analyses were performed on spectra utilizing curve fitting routines and conforming band positions using second derivatives and Fourier self-deconvolution techniques. The original spectrum and the inverted second derivative of the WPI/PEO 50:50 fiber sample are shown in Fig. 5(b) for illustrative purposes. This sample showed a strong absorption band in the Amide I region centered at 1644 cm^{-1} and an Amide II absorption band at 1542 cm^{-1}, which would indicate a high content of β-type structures and analysis of the band supports this observation. Curve resolution of the Amide I band (Fig. 5(c)) revealed that the protein secondary structure is approximately 12% α-helix, 38% β-sheet, 30% β-turn and 20% random coil. On the other hand, the 100% PEO fiber and powder samples, consistent with Fig. 5(a), showed no absorption in the amide I region between 1600 and 1700 cm^{-1}.

Fiber samples were compared by FTIR analyses of BLG:PEO at both neutral and acidic pH. Some differences are observed between the analyses of the WPI:PEO and BLG:PEO fiber samples prepared from neutral pH solutions, with shifts in both Amide I and II band peak maxima. This difference can be explained by the composition of WPI, which contains both ALA and BLG proteins. For comparison of fiber samples prepared from different pH, we used BLG as the protein component. The neutral pH BLG:PEO sample shows a peak maximum at 1632 cm^{-1} for the Amide I band and a strong Amide II band at 1535 cm^{-1} (Fig. 4(f)); while the acidic pH sample has similar Amide I and Amide II band peaks at 1633 cm^{-1} and 1535^{-1},

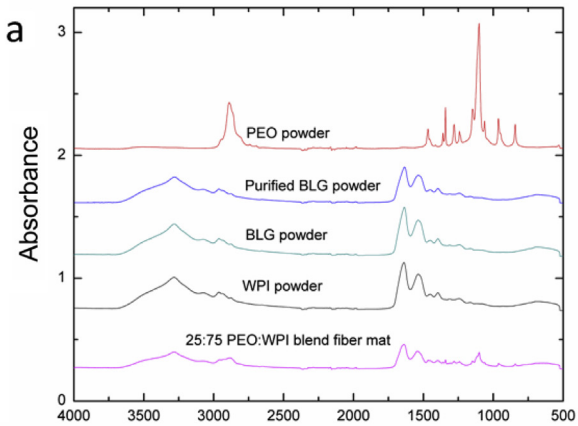

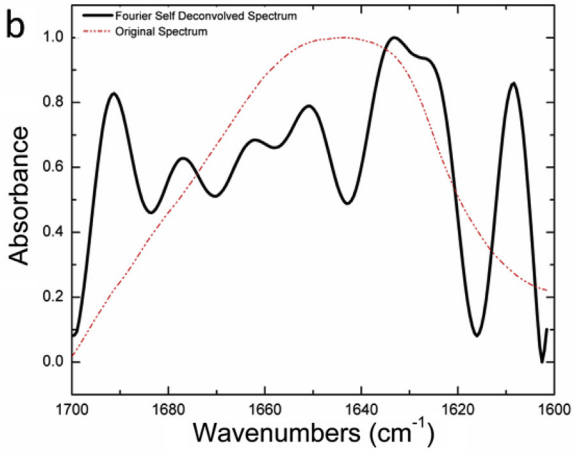

c

Sample	Peak position (cm^{-1})	Assignment	Peak position (cm^{-1})	Assignment
50:50 WPI:PEO	1616	β-sheet	1656	α-helix
	1624	β-sheet	1664	turns
	1634	β-sheet	1678	turns
	1647	unordered	1691	β-sheet

Fig. 5. (a) FTIR absorbance spectra for raw materials and representative PEO/WPI blend nanofiber mat; (b) Amide I Region of the 50:50 PEO:WPI sample showing the original spectrum and the Fourier self-deconvolved spectrum (Bandwidth 42 cm^{-1}, enhancement: 3.5); (c) Peak positions of the resolved Amide I region of whey protein isolate on PEO fibers. Protein secondary structure information for source material and nanofiber mats is given in Table 1.

respectively. The pH change induces only a slight change in overall conformation of the BLG:PEO samples based on this peak shift, which could be simply limited to measurement resolution and not a true shift. Secondary structural analysis of samples reveals small but significant changes in the overall conformation between neutral and acidic pH (Table 1). The overall trend indicates a higher helical and lower β-sheet content. At pH below the protein's isoelectric point, one would expect the protein to be highly protonated and therefore to exhibit more hydrogen bonding which could increase the percentage of helical character.

While FTIR analyses of the WPI/PEO blends shows the presence of both PEO and WPI in the mats as expected, perhaps of greater interest is the composition of the blend present on the surface of the fibers. In order to examine this issue x-ray photoelectron spectroscopy (XPS) was used to determine surface (<5 nm) constituents in atomic concentration. XPS survey scans utilizing PEO fiber mats with and without WPI are shown in Fig. 6. On the surface of the PEO fibers, both carbon and oxygen atoms are found as expected. In the WPI/PEO blend fiber, an additional nitrogen peak is observed, indicating the presence of whey protein on the fiber surface. The atomic nitrogen content on the surface of the fiber was approximately 10.6%, slightly higher than the theoretical 7.5% atomic nitrogen concentrated calculated based on the uniform bulk solution concentration. This suggests that the whey protein is more concentrated on the surface of the fiber which is consistent with previous studies by Sun et al. (2007).

XPS was also employed to examine the fiber mats made from BLG/PEO blends at various pH. Fig. 4(g) provides the atomic % of each element present on the nanofiber surface for each mat produced from acidic solution (pH 2.0), solution at the BLG isoelectric

Table 1
Conformational analysis of WP:PEO nanofiber sample protein secondary structure showing the effect of concentration, pH and dye addition. *BioPURE BLG used as received. pBLG is BioPURE BLG that has been purified.

Sample	β-sheet	α-helix	β-turn	Random coil
50:50 WPI:PEO (neutral pH) mat	38%	12%	30%	20%
75:25 WPI:PEO (neutral pH) mat	38%	16%	26%	20%
WPI powder	41%	12%	28%	19%
BLG* powder	43%	12%	26%	19%
Purified BLG powder	44%	11%	26%	19%
50:50 BLG*:PEO (neutral pH) mat	44%	12%	25%	19%
50:50 BLG*:PEO (pH 2) mat	36%	19%	24%	21%
50:50 pBLG:PEO with RhB mat	37%	15%	28%	20%

point (5.2) and approximately neutral solution (7.5). Oxygen concentration peaks at the isoelectric point, while nitrogen is at a minimum. The opposite effect is seen at pH 7.5, where nitrogen is nearly 2% higher than on the surface of the pH 5.2 fibers. Based on this, one could conclude that at the isoelectric point the BLG agglomerates with the more hydrophilic oxygen portions of the protein being on the surface of the fiber, while at pH 7.5, nitrogen is in higher quantity at the surface. At acidic pH, the nitrogen on the surface also is higher compared to that at the isoelectric point. Based on Tang et al.'s exploration of a similar spinnable polymer-protein system (PVA and BSA), we believe that at pH away from the BLG IEP, the PEO is drawn more to the surface of the Taylor cone and away from the fiber core by dielectrophoresis. Dielectrophoresis is movement of highest polarizable macromolecules in a fluid medium towards the non-uniform electric field's region of strongest intensity (Tang, Evren Ozcam, Stout, & Khan, 2012). At the BLG IEP, we conclude based on these XPS results that the PEO is more polarizable than the neutral BLG and is thus drawn more to the fiber surface than at alternative pH. Also, conformational changes of the BLG including a change from dimer to monomer expose a slightly increased amount of nitrogen. XPS results also indicate a new element present – chlorine – likely due to the lowering of solution pH using HCl solution. As shown in Fig. 4(g), sodium is present at the same order of magnitude in all three samples, indicating the possible presence of salt as a contaminant in the solution. The BLG used for these fiber preparations was purified, the PEO was not. Although some NaOH solution may have been used during the pH adjusting process of the pH 5.2 and 2.0 solutions, the pH 7.5 solution was not modified with NaOH.

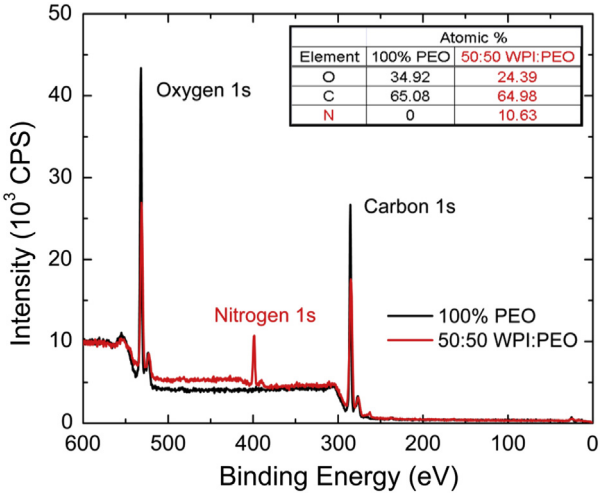

Fig. 6. An XPS survey scan is displayed for electrospun nanofibers generated from 4 w/w% PEO solutions with and without WPI. The inset table provides the atomic percent of each element present on the nanofiber mat surface.

3.4. Nanofiber heat treatment

We explored heat treatment to increase the thermal stability of the WP/PEO blend nanofibers, since covalently crosslinking of the whey protein is expected to occur upon heating above the gelation temperature. An enclosed vial containing BLG/PEO fiber sample was placed in a water bath at 80 °C for one hour. We used optical microscopy techniques (RLM and CLSM) to qualitatively examine the effect of heat treatment on the structure of the mats (Fig. 7 and TOC graphic). The PEO mat melts (Fig. 7(a)), while the blend fiber mats each retain a fibrous structure. The heat treated mats appear to transition from a molten state to a gel state with increasing WPI concentration. The 40:60 WPI:PEO mat shown in Fig. 7(b) and (e) looks very similar to the 50:50 WPI:PEO mat (image not shown).

Using electron microscopy, we looked more closely at the structure of the PEO fiber mats with (Fig. 8(a) and (b)) and without (Fig. 8(c) and (d)) BLG, both before and after this heat treatment. We observe that the fiber mat containing whey protein maintain both its fibrous structure and fiber diameter following heating (Fig. 8(a)). However, when the PEO-only fibers are heated to 80 °C, they melt to form a PEO film as shown in Fig. 8(d). Impressively, the addition of BLG to the blend and resultant fibers improves the stability and higher available surface area of the heated mat compared to a heated mat of 100% PEO. We also used XPS to evaluate changes in composition at the surface of the fiber after heat treatment. The atomic nitrogen concentration of the heat treated sample, measured using XPS, was 9.5%, which is slightly (~1.1%) lower than the fiber sample prior to heating. The decrease in the atomic nitrogen concentration was countered by an atomic oxygen concentration increase of 1.5%, while that of carbon stayed relatively constant, indicating that some conformational changes may have occurred to expose more oxygen laden portions of the amino acid chains. Additionally, mobility of PEO during heat treatment may explain the slight changes in atomic surface composition. This could lead to the development of a heat treatment process in order to control surface amino acid content taking advantage of this PEO mobility as well as the crosslinking occurring between denatured proteins. Nonetheless, even after heating, the protein is still on the fiber surface. This, along with the ability of the whey protein to permit the PEO fiber system to retain its fibrous-like network after heating above PEO's melting point could extend the potential of nanofibers to higher temperature applications as needed for food or other production processes that would require heating. Also, heating BLG increases the reactivity of its thiol group, especially above pH 7; thus, heat treating the WP:PEO blend mats could regulate their reactivity (Phillips, Whitehead, & Kinsella, 1994).

Thermal properties of the native and heat treated WP/PEO blend fiber mats were determined using DSC evaluation. Fig. 8(e) shows DSC thermograms of PEO, 50:50 purified BLG:PEO blend mats before and after heat treatment at 80 °C (of Fig. 8(b) and 9(a), respectively) and then the curve for purified BLG powder. According to Faridi-Majidi and Sharifi-Sanjani (2007), the intense melting peaks of each nanofiber mat indicates the presence of semi-crystalline products (Faridi-Majidi & Sharifi-Sanjani, 2007). We were able to examine the crystallinity of the WP/PEO blends. The crystallinity relative to crystalline PEO is calculated from $Xc(\%) = (\Delta H_f / \Delta H_f{}^o) \times 100$, where ΔH_f is the heat of fusion of the mat and $\Delta H_f{}^o$ is the heat of fusion of crystalline PEO (213.7 J/g) (Faridi-Majidi & Sharifi-Sanjani, 2007). Similar to Faridi-Majidi and Sharifi-Sanjani (2007), our PEO mat has a higher heat of fusion at 141.5 J/g than the blend mats, as well as a higher calculated nanofiber mat crystallinity of 66%. These values are lower than their powder PEO data (166.0 J/g; 77.68%) as expected. From this, we can similarly conclude that the PEO nanofiber production process

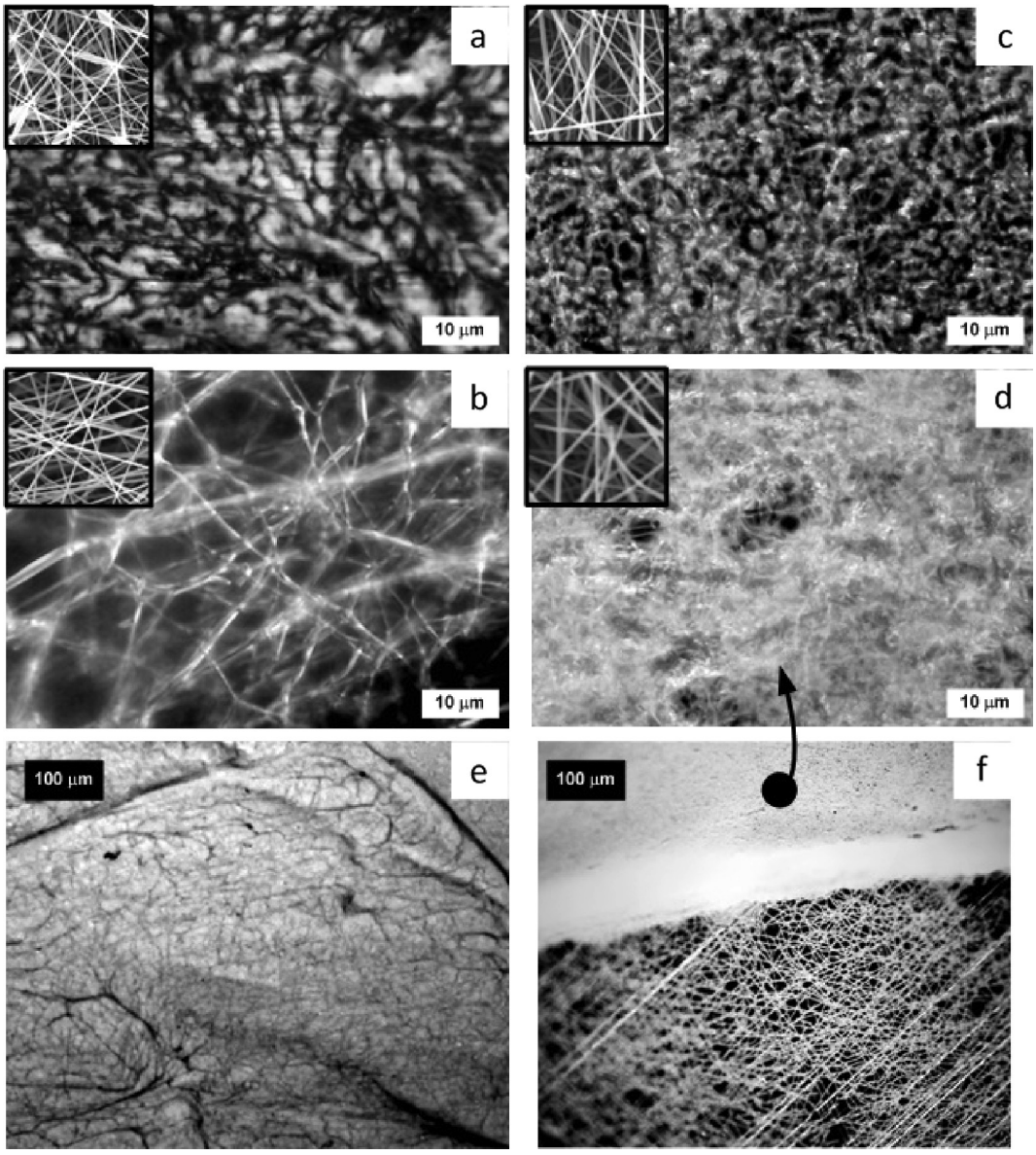

Fig. 7. Reflected light dark field microscope images of heat treated whey protein isolate (WPI) and poly(ethylene oxide) (PEO) blend solution electrospun nanofiber mats. PEO 4 w/w % with increasing WPI concentration, with WPI:PEO ratio (a) 0:100; (b) 40:60; (c) 60:40; (d) 75:25. Insets in (a)–(d) are SEM images of original mats (before heat treatment) at same scale as reflected light microscope images. (e) is reflected light image of (b) 40:60 WPI:PEO at lower magnification, showing melt appearance; while (f) is reflected light image of (d) 75:25 WPI:PEO at lower magnification, showing networked fiber gel appearance with thinner fibrous sample edge that was formed from pulling mat apart.

reduces its crystallinity (Faridi-Majidi & Sharifi-Sanjani, 2007). The addition of the WP to the formulation significantly reduces this relative crystallinity to 22–27%. We also note that the addition of BLG to the PEO nanofibers lowers the melting point of the mat compared to PEO from 67 °C to 55 °C, which indicates that the ability of the BLG to form some bonds at it is heated to above its denaturation temperature (approximately 71 °C) (Phillips et al., 1994). The addition of BLG to the PEO nanofibers lowers the melting point of the mat compared to an all PEO (from 67 °C to 55 °C), but a heat treatment of the mat will increase that melting point to 62 °C. Similarly, as shown in Fig. 8(f), blending WPI in the PEO mat formulation will decrease the melting point, but heat treatment of this mat even further lowers its melting point. This is likely due to the presence of ALA and other proteins in the WPI blend which do not crosslink upon heating like the purified BLG (Fig. 8(g)).

3.5. Incorporation and release of a small molecule

As an initial step towards using these WP/PEO blend fibers as potential delivery vehicles, we incorporated and examined the release of a water soluble dye molecule Rhodamine B (RhB). We conducted a qualitative visual study to determine the distribution of RhB in PEO nanofibers with or without the addition of BLG to the solution prior to electrospinning. To do this, we examined the fibers containing RhB with SEM and CLSM (Fig. 9). At 4 w/w% in water with 0.02 w/w% RhB, PEO forms beaded nanofibers as shown in Fig. 9(a) with fibers “bunched” in the mat, possibly due to dye clusters. The corresponding confocal microscopic image in Fig. 9(b) shows brighter areas of dye near voids where these bunches or clusters have formed. The fiber mat electrospun from solution containing an additional 4 w/w% purified BLG in Fig. 9(c) does not contain the presence of these clusters on the confocal image

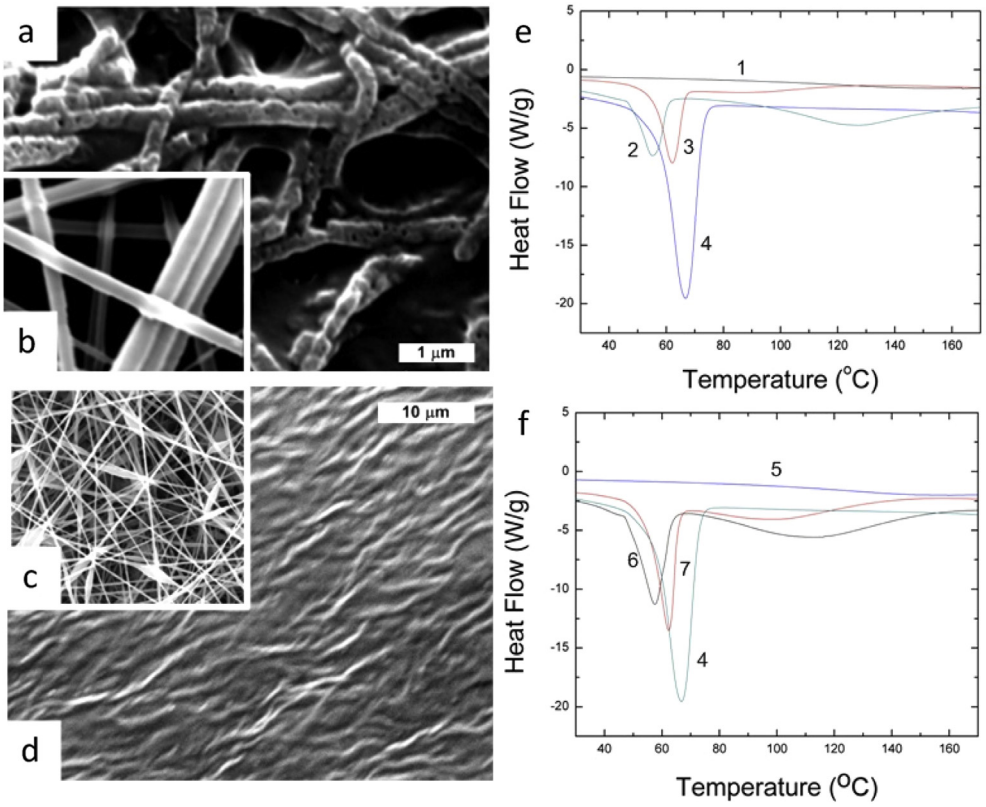

g

Sample composition	prior heat treatment at 80 °C?	melting point (° C)	ΔHf (J/g)	Xc (%)
100% PEO (4)	no	66.82	141.50	66%
50:50 PEO:pBLG (2)	no	55.12	48.63	23%
50:50 PEO:pBLG (3)	yes	62.07	49.11	23%
50:50 PEO:WPI (7)	no	62.38	56.76	27%
50:50 PEO:WPI (6)	yes	57.51	46.43	22%

Fig. 8. Scanning electron microscope images of 8 w/w% purified BLG (pBLG)/PEO blend nanofibers (a) after and (b) before (inset) heat treatment at 80 °C; PEO nanofibers (c) before (inset) and (d) after heat treatment at 80 °C. Images (a) and (b) are at same scale; as are (c) and (d). (e) and (f) provide DSC thermographs of nanofiber mats and powders: scan (1) purified BLG (pBLG) powder; (2) pBLG:PEO 50:50 native nanofiber mat (b); (3) pBLG:PEO 50:50 heat treated nanofiber mat (a); (4) PEO nanofiber mat (c); (5) BiPRO WPI powder; (6) WPI:PEO 50:50 heat treated nanofiber mat; (7) WPI:PEO 50:50 native nanofiber mat; (g) summarizes DSC data.

(Fig. 9(d)) indicating, qualitatively, a more uniform distribution of dye. Thus, the BLG addition to solution appeared to improve the uniformity of the fiber mat as well as the distribution of the model flavonoid molecule RhB. FTIR comparison between the RhB–BLG–PEO, BLG–PEO and WPI–PEO blend fibers showed no strong difference or additional peaks (data not shown). However, secondary structure of the BLG was slightly affected by the presence of RhB (Table 1). This indicates that incorporating a molecule into a protein-based nanofiber system may influence protein secondary structure, but may not influence system performance. This would require evaluating each protein and delivery-molecule system.

Release of RhB from both PEO and BLG/PEO blend into DI water at room temperature was monitored over several minutes. In both cases, approximately 90% of the RhB was released within 10 min. Interestingly, despite the difference in distribution of the dye within the PEO and BLG/PEO fiber mats, there was no significant difference in the release profiles (Fig. 10(d)) and samples were dissolving.

In order to establish an insoluble nanofiber mat of these materials, we heat treated mats of PEO and BLG/PEO for 24–44 h at 100 °C (Fig. 10(a)), which is well above the gelation temperature of the WP and above the melting point of PEO. After heat treatment,

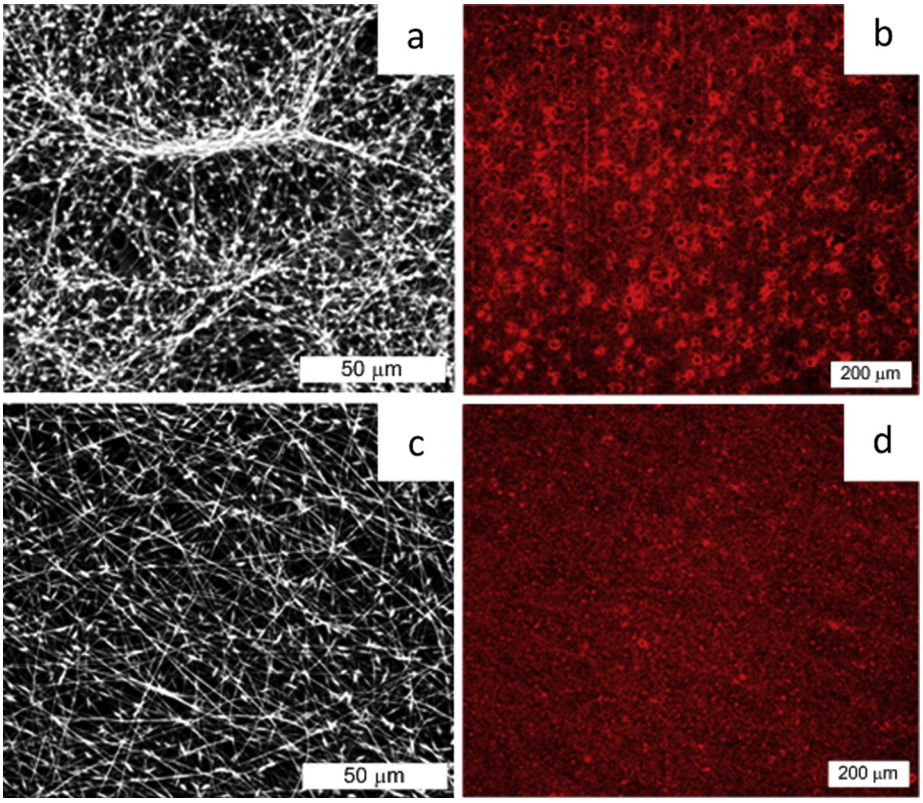

Fig. 9. PEO fiber mat with 4 w/w% PEO and 0.02% RhB in deionized water *without* BLG (a) scanning electron micrograph, (b) confocal microscope image of RhB distribution; and *with* BLG (50:50 BLG:PEO for total 8 w/w%) (c) scanning electron micrograph, (d) confocal microscope image of RhB distribution.

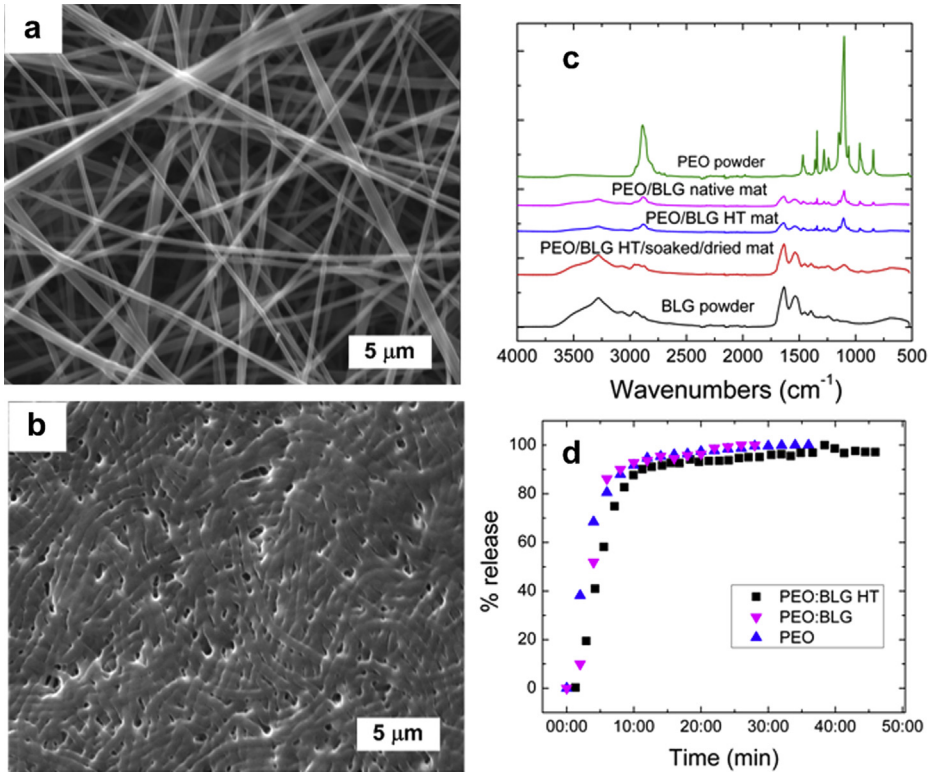

Fig. 10. PEO:BLG (50:50 BLG:PEO for total 8 w/w%) blend fiber mat (a) post heat treatment at 100 °C for 18 h, (b) post heat treatment then after soaking in water and air drying, (c) FTIR comparison between native, heat treated, heat treated/immersed/dried mats and raw material powder, (d) release of RhB over time from fiber mat samples of PEO, BLG:PEO and heat treated BLG:PEO.

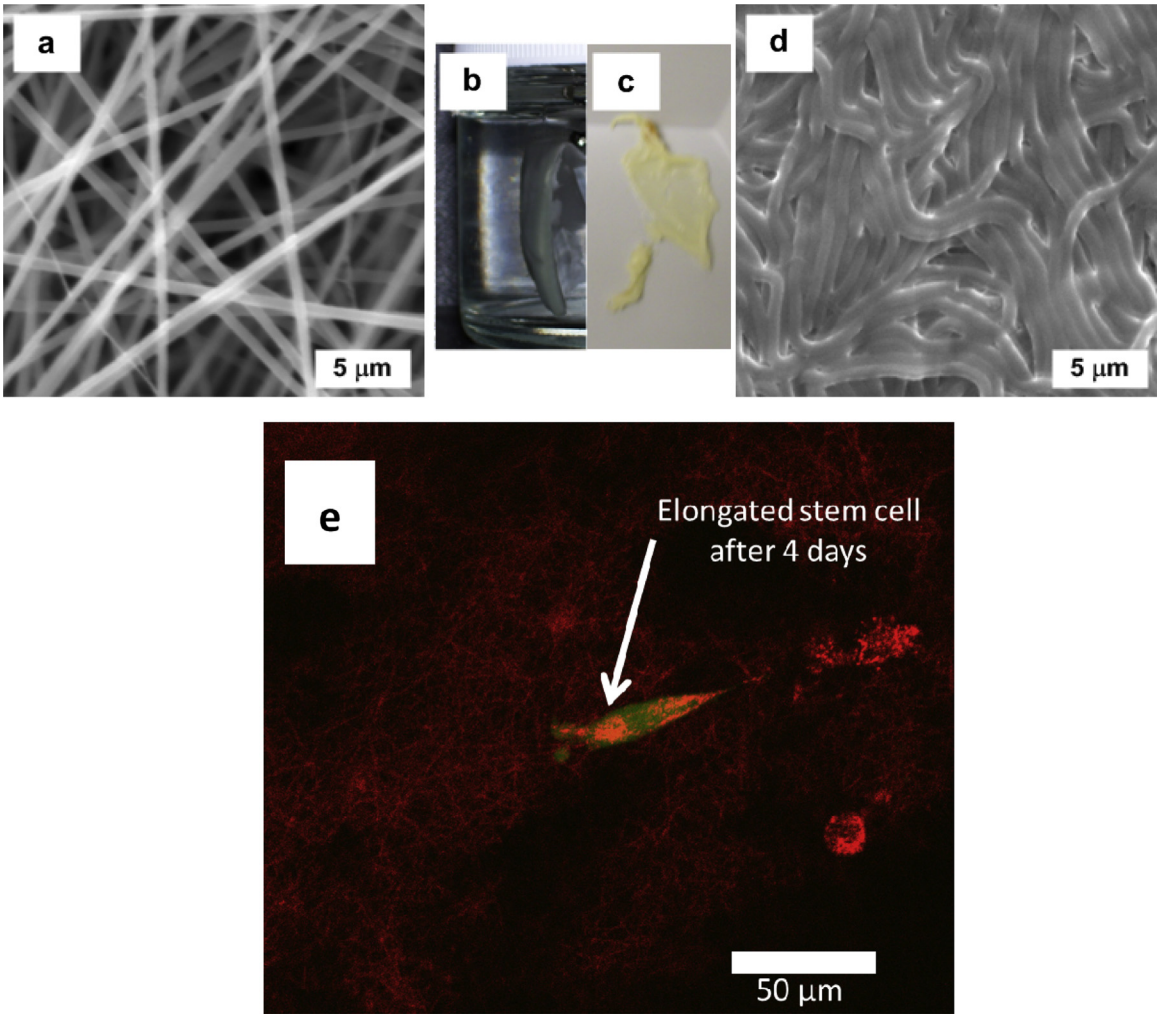

Fig. 11. PEO:WPI (25:75 for total 16 w/w%) nanofiber mat with post heat treatment at 100 °C for 44 h (a) post heat treatment, (b) suspended soaking in deionized water, (c) sample removed from water soak, (d) SEM of sample (c) air dried and sputter coated with gold. In (e), a heat treated BLG/PEO nanofiber mat serves as successful scaffold for stem cell proliferation. (For interpretation of the references to color in this figure legend, the reader is referred to the web version of this article.)

we found that the mats did not dissolve even after days of soaking in water and ultimately air drying (Fig. 10(b)), since we believe the protein crosslinks during the heat treatment. However, the mats did not return to their original state after soaking and drying, possibly since much of the PEO may be free to dissolve. Release of RhB from the heat treated mat (Fig. 10(d)) is slightly slower compared to its counterparts possibly because the mat is not dissolving in this case. Nevertheless this formulation would still fall in the "immediate release" category as RhB is released in minutes and not hours. However, what this does show is that a heat treated mat, being insoluble, could serve as a wound dressing for release of an active pharmaceutical ingredient.

We examined the FTIR spectra after electrospinning, heat treatment, and soaking in water (data shown for the PEO/BLG blend (Fig. 10(c))). While no difference in the spectra is seen between the native and heat treated mat, we believe that after exposure to water the majority of the PEO dissolves and the mat appears to be predominantly whey protein as indicated by the changes in the peak at approximately 1250 cm^{-1}. Results for the WPI/PEO blend mats were similar to that for the BLG/PEO. Fig. 11(a) provides SEM image of the original heat treated mat, (b) this sample suspended and soaking in water, (c) sample after removal from water and (d) the dry, post-soaking mat under SEM. The sample in Fig. 11(b) swelled with a minimum swelling ratio of 5.7 ($=(m - m_o)/m_o$) where m_o is initial sample mass and m is mass after soaking) after removal from water and blot dry with filter paper). The success of heat treatment we found depended on heat treatment time and sample thickness (data not shown). For example, the same sample heat treated 18 h dissolved in water immediately; while after 44 h it swelled and maintained stability in water as shown in Fig. 11(b)–(d). In general we believe that during heat treatment of the PEO:WP fiber mats, as the PEO melts (above 60 °C), the BLG unfolds and forms disulfide bonds resulting in crosslinks in and between fibers. Further work has moved these heat treated WP:PEO fiber mats to the tissue engineering laboratory as a variant to other biopolymer scaffolding options (Vlierberghe, Dubruel, & Schacht, 2011). Fig. 11(e) shows the growth of a cardiac stem cell on a BLG–PEO composite mat, and is a topic of further study.

4. Conclusions

In this study, we demonstrated fabrication of electrospun nanofibers from whey proteins (WP) and its component beta lactoglobulin (BLG). Aqueous whey protein solutions either in native or denatured form yielded interesting micro and structures; while the addition of poly(ethylene oxide) to the system led to

bead-free nanofiber formation. Nanofibers with WP:PEO composition as high as 3:1 could be obtained with diameters ranging between 312 and 690 nm depending on composition and total polymer concentration. Further, WP/PEO blends at a pH of 2.0 could be electrospun, which is desirable for reduced bacterial growth and increased product shelf life. However, beaded nanofibers resulted near the isoelectric point (pH ~ 5) possibly from protein aggregation. XPS analysis of the blend fibers confirmed the presence of the protein and showed whey proteins were more concentrated on the fiber surface than the bulk. FTIR analysis also confirmed the presence, and revealed the secondary structure changed as a function of pH. Heat treatment of the blend fibers using temperatures above the gelation temperature of the protein increased the thermal stability of the fibers and with prolonged heat treatment, enabled the mat to become less soluble in water primarily due to the WP crosslinks. This heat treatment and resultant soaking mat stability shows promise for various applications and is subject of ongoing work.

Acknowledgments

We thank Davisco Foods International, Inc. for providing the BiPRO and BetaLAC whey protein products. We acknowledge the help of Dr. Jason Bond, Dr. Thomas Fink and the East Carolina University (ECU) Biology Department Imaging Core for Scanning Electron Microscope utilization and Mr. Chris Dunkley of Olympus for reflected light microscopy support. We also thank the Dr. Orlin Velev group at North Carolina State University for assistance with initial confocal microscopy. We are grateful to East Carolina University students H. Ray Tichenor, Jamelle Simmons, Joseph A. Rose, Clayton D. Rice, Adam Hussaini, and Thomas A. Deaton for support of this work. We thank and look forward to continued collaboration with Dr. Barbara Muller-Borer and Maria Collins of the ECU Cell-Based Therapy & Tissue Engineering Lab.

Appendix A. Supplementary data

Supplementary data related to this article can be found at http://dx.doi.org/10.1016/j.foodhyd.2013.07.023.

References

Alting, A. C., Weijers, M., deHoog, E. H. A., vandePijpekamp, A. M., CohenStuart, M. A., Hamer, R. J., et al. (2004). Acid-induced cold gelation of globular proteins: effects of protein aggregate characteristics and disulfide bonding on rheological properties. *Journal of Agricultural and Food Chemistry, 52*(3), 623–631.

Andrady, A. L. (2008). *Science and technology of polymer nanofibers*. NY: Wiley.

Anema, S. G. (2008). Effect of milk solids concentration on the gels formed by the acidification of heated pH-adjusted skim milk. *Food Chemistry, 108*(1), 110–118.

Bertrand, M., & Turgeon, S. L. (2007). Improved gelling properties of whey protein isolate by addition of xanthan gum. *Food Hydrocolloids, 21*(2), 159–166.

Boudriot, U., Dersch, R., Greiner, A., & Wendorff, J. H. (2006). Electrospinning approaches toward scaffold engineering – a brief overview. *Artificial Organs, 30*(10), 785–792.

Chandan, R. C (2006). Milk composition, physical and processing characteristics. In R. C. Chandan (Ed.), *Manufacturing Yogurt and Fermented Milks* (pp. 311–325). Ames, IA: Blackwell Publishing.

Chandan, R. C., & Shah, N. P. (2006). Functional foods and disease prevention. In R. C. Chandan (Ed.), *Manufacturing Yogurt and Fermented Milks* (pp. 311–325). Ames, IA: Blackwell Publishing.

Chatterton, D. E. W., Smithers, G., Roupas, P., & Brodkorb, A. (2006). Bioactivity of β-lactoglobulin and α-lactalbumin: technological implications for processing. *International Dairy Journal, 16*(11), 1229–1240.

Choi, J. S., & Yoo, H. S. (2007). Electrospun nanofibers surface-modified with fluorescent proteins. *Journal of Bioactive and Compatible Polymers, 22*, 508–524.

Cui, W., Zhou, Y., & Chang, J. (2010). Electrospun nanofibrous materials for tissue engineering and drug delivery. *Science and Technology of Advanced Materials, 11*(1), 014108.

Daubert, C. R., Hudson, H. M., Foegeding, E. A., & Prabhasankar, P. (2006). Rheological characterization and electrokinetic phenomena of charged whey protein dispersions of defined sizes. *LWT – Food Science and Technology, 39*(3), 206–215.

Dror, Y., Ziv, T., Makarov, V., Wolf, H., Admon, A., & Zussman, E. (2008). Nanofibers made of globular proteins. *Biomacromolecules, 9*, 2749–2754.

Eissa, A. S., Bisram, S., & Khan, S. A. (2004). Polymerization and gelation of whey protein isolates at low pH using transglutaminase enzyme. *Journal of Agricultural and Food Chemistry, 52*, 4456–4464.

Eissa, A. S., & Khan, S. A. (2005). Acid induced gelation of preheated, enzymatically modified whey proteins. *Journal of Agricultural and Food Chemistry, 53*(12), 5010–5017.

Eissa, A. S., & Khan, S. A. (2006). Modulation of hydrophobic interactions in denatured whey proteins by transglutaminase enzyme. *Food Hydrocolloids, 20*(4), 543–547.

Eissa, A. S., Puhl, C., Kadla, J. F., & Khan, S. A. (2006). Enzymatic cross-linking of β-lactoglobulin: conformational properties using FTIR spectroscopy. *Biomacromolecules, 7*(6), 1707–1713.

Errington, A. D., & Foegeding, E. A. (1998). Factors determining fracture stress and strain of fine-stranded whey protein gels. *Journal of Agricultural and Food Chemistry, 46*, 2963–2967.

Faridi-Majidi, R., & Sharifi-Sanjani, N. (2007). In situ synthesis of iron oxide nanoparticles on poly(ethylene oxide) nanofibers through an electrospinning process. *Journal of Applied Polymer Science, 105*(3), 1351–1355.

Frenot, A., & Chronakis, I. S. (2003). Polymer nanofibers assembled by electrospinning. *Current Opinion in Colloid and Interface Science, 8*, 64–75.

Ha, E., & Zemel, M. B. (2003). Functional properties of whey, whey components, and essential amino acids: mechanisms underlying health benefits for active people (review). *The Journal of Nutritional Biochemistry, 14*(5), 251–258.

Huang, Z., Zhang, Y.-Z., Kotaki, M., & Ramakrishna, S. (2003). A review on polymer nanofibers by electrospinning and their applications in nanocomposites. *Composites Science and Technology, 63*, 2223–2253.

Ignatious, F., & Sun, L. (2006). *Electrospun amorphous pharmaceutical compositions*. US Patent 2006013869-A1.

Ignatious, F., Sun, L., Lee, C., & Baldoni, J. (2010). Electrospun nanofibers in oral drug delivery. *Pharmaceutical Research, 27*(4), 576–588.

International Commission for the Microbiological Specifications for Foods. (1998). *Microorganisms in foods 6. Microbial ecology of food commodities*. Blackie Academic and Professional.

Jia, H., Zhu, G., Vugrinovich, B., Kataphinan, W., Reneker, D. H., & Wang, P. (2002). Enzyme-carrying polymeric nanofibers prepared via electrospinning for use as unique biocatalysts. *Biotechnology Progress, 18*(5), 1027–1032.

Jiang, H., Hu, Y., Li, Y., Zhao, P., Zhu, K., & Chen, W. (2005). A facile technique to prepare biodegradable coaxial electrospun nanofibers for controlled release of bioactive agents. *Journal of Controlled Release, 108*(2–3), 237–243.

Jin, H., Fridrikh, S. V., Rutledge, G. C., & Kaplan, D. L. (2002). Electrospinning bombyx mori silk with poly(ethylene oxide). *Biomacromolecules, 3*, 1233–1239.

Jung, J., Savin, G., Pouzot, M., Schmitt, C., & Mezzenga, R. (2008). Structure of heat-induced β-lactoglobulin aggregates and their complexes with sodium-dodecyl sulfate. *Biomacromolecules, 9*(9), 2477–2486.

Katti, D. S., Robinson, K. W., Ko, F. K., & Laurencin, C. T. (2004). Bioresorbable nanofiber-based systems for wound healing and drug delivery: optimization of fabrication parameters. *Journal of Biomedical Materials Research Part B: Applied Biomaterials, 70B*, 286–296.

Kim, S. H., Nam, Y. S., Lee, T. S., & Park, W. H. (2003). Silk fibroin nanofiber. Electrospinning, properties and structure. *Polymer Journal, 35*(2), 185–190.

Kowalczyk, T., Nowicka, A., Elbaum, D., & Kowalewski, T. A. (2008). Electrospinning of bovine serum albumin. Optimization and the use for production of biosensors. *Biomacromolecules, 9*(7), 2087–2090.

Kriegel, C., Arrechi, A., Kit, K., McClements, D. J., & Weiss, J. (2008). Fabrication, functionalization, and application of electrospun biopolymer nanofibers. *Critical Reviews in Food Science and Nutrition, 48*, 775–797.

Li, D., & Xia, Y. (2004). Electrospinning of nanofibers: reinventing the wheel? *Advanced Materials, 16*, 1151–1170.

Li, M., Mondrinos, M. J., Gandhi, M. R., Ko, F. K., Weiss, A. S., & Lelkes, P. I. (2005). Electrospun protein fibers as matrices for tissue engineering. *Biomaterials, 26*, 5999–6008.

Li, W., Laurencin, C. T., Caterson, E. J., Tuan, R. S., & Ko, F. K. (2002). Electrospun nanofibrous structure: a novel scaffold for tissue engineering. *Journal of Biomedical Materials Research, 60*, 613–621.

Little, R. C., & Ting, R. Y. (1976). *Journal of Chemical and Engineering Data, 21*, 422–423.

Livney, Y. D. (2010). Milk proteins as vehicles for bioactives. *Current Opinion in Colloid and Interface Science, 15*(1–2), 73–83.

Madureira, A. R., Pereira, C. I., Gomes, A. M. P., Pintado, M. E., & Malcata, F. X. (2007). Bovine whey proteins – overview on their main biological properties. *Food Research International, 40*(10), 1197–1211.

MaHam, A., Tang, S., Wu, H., Wang, J., & Lin, Y. (2009). Protein-based nanomedicine platforms for drug delivery. *Small, 5*(15), 1706–1721.

Mailliart, P., & Ribadeau-Dumas, B. (1988). Preparation of β-lactoglobulin and β-lactoglobulin-free proteins from whey retentate by sodium chloride salting out at low pH. *Journal of Food Science, 53*(3), 743–752.

Manasco, J. L., Saquing, C. D., Tang, C., & Khan, S. A. (2012). Cyclodextrin fibers via polymer-free electrospinning. *RSC Advances, 2*(9), 3778–3784.

Min, B., Lee, G., Kim, S. H., Nam, Y. S., Lee, T. S., & Park, W. H. (2004). Electrospinning of silk fibroin nanofibers and its effect on the adhesion and spreading of normal human keratinocytes and fibroblasts in vitro. *Biomaterials, 25*(7–8), 1289–1297.

Miyoshi, T., Toyohara, K., & Minematsu, H. (2005). Preparation of ultrafine fibrous zein membranes via electrospinning. *Polymer International, 54*, 1187–1190.

Nie, H., He, A., Zheng, J., Xu, S., Li, J., & Han, C. C. (2008). Effects of chain conformation and entanglement on the electrospinning of pure alginate. *Biomacromolecules, 9*(5), 1362–1365.
Phillips, L. G., Whitehead, D. M., & Kinsella, J. (1994). *Structure–function properties of food proteins*. London: Academic Press.
Saquing, C. D., Manasco, J. L., & Khan, S. A. (2009). Electrospun nanoparticle-nanofiber composites via a one-step synthesis. *Small, 5*(8), 944–951.
Satpathy, G., & Rosenberg, M. (2003). Encapsulation of chlorothiazide in whey proteins: effects of wall-to-core ratio and cross-linking conditions on microcapsule properties and drug release. *Journal of Microencapsulation, 20*(2), 227.
Socrates, G. (1994). *Infrared characteristic group frequencies: Tables and charts* (2nd ed.). Chichester: John Wiley & Sons.
Son, W. K., Youk, J. H., Lee, T. S., & Park, W. H. (2005). Effect of pH on electrospinning of poly(vinyl alcohol). *Materials Letters, 59*(12), 1571–1575.
Son, W. K., Youk, J. H., Lee, T. S., & Park, W. H. (2004). The effects of solution properties and polyelectrolyte on electrospinning of ultrafine poly(ethylene oxide) fibers. *Polymer, 45*(9), 2959–2966.
Song, J., Kim, H., & Kim, H. (2008). Production of electrospun gelatin nanofiber by water-based co-solvent approach. *Journal of Materials Science: Materials in Medicine, 19*, 95–102.
Srikar, R., Yarin, A. L., Megarides, C. M., Bazilevsky, A. V., & Kelley, E. (2008). Desorption-limited mechanism of release from polymer nanofibers. *Langmuir, 24*, 965–974.
Sun, X.-Y., Shankar, R., Börner, H. G., Ghosh, T. K., & Spontak, R. J. (2007). Field-driven biofunctionalization of polymer fiber surfaces during electrospinning. *Advanced Materials, 19*, 87–91.
Talwar, S., Hinestroza, J., Pourdeyhimi, B., & Khan, S. A. (2008). Associative polymer facilitated electrospinning of nanofibers. *Macromolecules, 41*(12), 4275–4283.
Tang, C., Evren Ozcam, A., Stout, B., & Khan, S. A. (2012). Effect of pH on protein distribution in electrospun PVA/BSA composite nanofibers. *Biomacromolecules, 13*, 1269–1278.
Torres-Giner, S., Gimenez, E., & Lagaron, J. M. (2008). Characterization of the morphology and thermal properties of zein prolamine nanostructures obtained by electrospinning. *Food Hydrocolloids, 22*(4), 601–614.
Vega-Lugo, A., & Lim, L. (2012). Effects of poly(ethylene oxide) and pH on the electrospinning of whey protein isolate. *Journal of Polymer Science Part B: Polymer Physics, 50*(16), 1188–1197.
Vlierberghe, S. V., Dubruel, P., & Schacht, E. (2011). Biopolymer-based hydrogels as scaffolds for tissue engineering applications: a review. *Biomacromolecules, 12*(5), 1387–1408.
Wnek, G. E., Carr, M. E., Simpson, D. G., & Bowlin, G. L. (2003). Electrospinning of nanofiber fibrinogen structures. *Nano Letters, 3*(2), 213–216.
Woerdeman, D. L., Shenoy, S., & Breger, D. (2007). Role of chain entanglements in the electrospinning of wheat protein-poly(vinyl alcohol) blends. *The Journal of Adhesion, 83*, 785–798.
Woerdeman, D. L., Ye, P., Shenoy, S., Parnas, R. S., Wnek, G. E., & Trofimova, O. (2005). Electrospun fibers from wheat protein: investigation of the interplay between molecular structure and the fluid dynamics of the electrospinning process. *Biomacromolecules, 6*, 707–712.
Wongsasulak, S., Kit, K. M., McClements, D. J., Yoovidhya, T., & Weiss, J. (2007). The effect of solution properties on the morphology of ultrafine electrospun egg albumen – PEO composite fibers. *Polymer, 48*(2), 448–457.
Xie, J., & Hsieh, Y. (2003). Ultra-high surface fibrous membranes from electrospinning of natural proteins: casein and lipase enzyme. *Journal of Materials Science, 38*(10), 2125–2133.
Yang, J., Ichii, T., Murase, K., & Sugimura, H. (2012). Circular arrays of gold nanoparticles of a single particle line thickness formed on indium tin oxide. *Applied Physics Express, 5*(2), 025202. http://dx.doi.org/10.1143/APEX.5.025202.
Yi, F., Guo, Z., Fang, Z., Yu, J., & Li, Q. (2004). Mimetics of eggshell membrane protein fibers by electrospinning. *Macromolecular Rapid Communications, 25*, 1038–1043.
Zeng, J., Aigner, A., Czubayko, F., Kissel, T., Wendorff, J. H., & Greiner, A. (2005). Poly(vinyl alcohol) nanofibers by electrospinning as a protein delivery system and the retardation of enzyme release by additional polymer coatings. *Biomacromolecules, 6*, 1484–1488.
Zhong, H., Gilmanshin, R., & Callender, R. (1999). An FTIR study of the complex melting behavior of α-lactalbumin. *Journal of Physical Chemistry B, 103*(19), 3947–3953.
Zhu, J., Shao, H., & Hu, X. (2007). Morphology and structure of electrospun mats from regenerated silk fibroin aqueous solutions with adjusting pH. *International Journal of Biological Macromolecules, 41*(4), 469–474.
Zoccola, M., Montarsolo, A., Aluigi, A., Varesano, A., Vineis, C., & Tonin, C. (2007). Electrospinning of polyamide 6/modified-keratin blends. *E-Polymers*, (105), 1–19.